Electron Transfer between Metal Ions and Photoexcited Semiconductors

K. Katsiev and H. Idriss*

ABSTRACT: Electron transfer between metal ions and excited solid materials is central to many catalytic events in natural and synthetic systems. The interaction of metal ions, leading to their reduction, with the excited semiconductor is expected to decrease the lifetime of excited electrons and increase that of the holes. By conducting this reaction using a semiconductor single crystal [rutile TiO_2 (110)] in the aqueous phase and the presence of different Ag^+ concentrations, it was found that the initial signal of excited electrons increases and the signal related to holes decreases, which is the opposite of expectations. Results indicate that this is most likely related to the initial interaction, the adsorption process (surface O_{GS}−Ag^+; GS: ground state) that precedes the electron transfer reaction (Ti_{ex}^{3+}−Ag metal; ex: excited state). Similar results are obtained for the Ce^{4+} interaction with the surface of TiO_2(110).

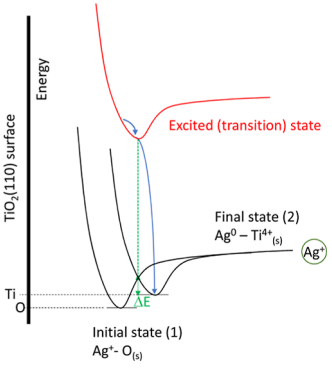

INTRODUCTION

Electron transfer between two interacting systems is central to most chemical reactions. While considerable knowledge is available for the interaction of two ionic systems in the liquid phase,[1] the temporal nature of the electronic interaction of metal ions with the surface of oxide semiconductors in an aqueous environment is largely unknown. Interactions leading to electron transfer between two ionic complexes are well described by Marcus' and other similar theories,[2] in which the reorganization energy has a central role because it slows down the fast electron transfer between two given ions. The situation is different when an ion interacts with a surface. This is because the surface of a solid represents an infinite size compared to the ions and is therefore largely static. As a consequence, unlike the interaction between two ions in solution, the ionic interaction with an excited solid semiconductor, before the charge transfer event, is poised to be governed by the nature of the adsorption of the given ion. In this case, and in the absence of a photon, it is largely a result of the electrostatic potential between the ion and the surface site.[3] This is because, in this step, no charge has been transferred. In the case of a metal oxide, the interaction occurs between the surface O atoms (high electron density) and the metal ions in solution. Strictly, the surface is hydroxylated in an aqueous phase, but this would not change the nature of the adsorption because the surface hydroxyl still contains high electron density[4] around the O atom. For example, a recent experimental and computational study has shown that Ag^+ interacts with the oxygen and nitrogen anions of the metal−organic framework.[5] The situation will change upon light excitation, where electron transfer occurs from the valence band (VB) to the conduction band (CB) within the semiconductor. In the case of a semiconductor with no electrons in the d-orbitals, such as TiO_2, the transfer occurs from O 2p orbitals to Ti 3d orbitals. As a result, holes reside on the O atom and electrons on the Ti atom.[6] In other words, the temporal electron distribution on the two centers is reversed. This would affect the position of the metal ions adsorbed on an O atom. Adsorbed ions will move from the O atom centers on which they reside, due to the electrostatic repulsion with the holes, toward Ti atoms, due to electrostatic attraction with the excited electrons, and where they get reduced. This type of interaction may be monitored by pump−probe transient absorption spectroscopy (TAS).

In the case of oxide semiconductors excited with energy higher than their bandgap, there are generally three observed regions by TAS. The first is at the bandgap energy where a negative signal is viewed as evidence of depleted VB electrons in the excited state, ground-state bleaching (GSB), although this has seldom been seen in the case of TiO_2. The second is a positive signal in the visible region commonly attributed to holes.[7] The third, also a positive signal, is in the IR region, attributed to trapped electrons[8] and polarons (self-trapped excited electrons).[9] Both the second and the third are commonly called photon-inducted absorption (IPA).

To conduct the experiment, we used the most studied and probably understood n-type oxide semiconductor single crystal, the rutile TiO_2(110), as a prototype.[10−12] The use of a single crystal is important as it removes possible effects of grain boundary,[13] degree of crystallinity,[14] and multiple surface orientations,[15] among other factors. All affect the performance of polycrystalline photocatalysts and are poised to affect the TAS signal. The reaction is conducted in solution to mimic the solid−liquid aqueous environment encountered in nature. The metal cation used is Ag^+, which is one of the simplest reducible cations to Ag metal by excited electrons and is used to generate O_2 from water upon trapping excited electrons from the CB.[16] This allows for holes to be transferred to adsorbed water molecules, making O_2 and protons.

EXPERIMENTAL SECTION

The setup of TAS consists of a regeneratively amplified Ti:sapphire laser system that produces 800 nm laser pulses of 90 fs pulse width at 1 kHz repetition rate in conjunction with ExciPro pump−probe spectrometers (CDP, Moscow). Pump pulses (320 nm) were generated after passing through 90% of the 800 nm beam into a spectrally tunable (240−2600 nm) optical parametric amplifier (Spectra-Physics) and a frequency mixer (NIR Vis UV, Light conversion). The fluency of the pump power was about 15 mW/cm^2. To generate the probe pulses (UV, visible, and NIR wavelength continuum), the remaining 10% of the 800 nm amplified pulses were focused onto a CaF_2 crystal. To study the transient signal following excitation, the 800 nm amplified pulses were passed through a motorized delay stage before white light generation. The pump pulses (320 nm) and the probe light were overlapped on the TiO_2 (110) single crystal and then reflected with a mirror to the detector. The pump pulses passed through a synchronized chopper (500 Hz), which blocked alternative pump pulses. The experiments were carried out in a reactor constructed around a standard 10 mm optical-path quartz cuvette. A fresh TiO_2 single crystal (10 × 5 mm^2) (from MTI) was used. The fresh sample was cleaned with ethanol in an ultrasound bath and then dried in ambient conditions. The crystal was positioned vertically, normal to the pump/probe laser beams, enabling the measurements in reflection mode. The cuvette was filled with deionized water (Milli Q filtration) and sealed with a reclosable plastic cap with a rubber seal (3D-printed). The cap was equipped with two syringe needles for N_2 purging and introduction of the reactants. Silver nitrate was dissolved in water to a 6 × 10^{-3} M concentration and added to the reactor dropwise with a microliter droplet volume through one of the needles by a syringe. The change in absorption (ΔA) of the excited state is calculated by subtracting the absorption of the excited sample from the unexcited sample.

RESULTS AND DISCUSSION

It was observed that the presence of Ag^+ resulted in increasing the short (<10 ps) lifetime of excited electrons in the CB and decreasing the lifetime of trapped holes. This was contrary to expectation because Ag^+ is ultimately reduced to Ag^0, and one would expect that it would decrease the lifetime of excited electrons and consequently increase that of holes (because of a decreased electron−hole recombination rate). Figure S1 presents the TAS signal of TiO_2(110) when Ag^+ was added at two different concentrations (A and B) in the UV and visible regions. GSB became pronounced in the presence of Ag^+. The appearance of GSB is because, by trapping electrons from the CB, the excited state has fewer VB electrons and this leads to a negative signal. Also shown in Figure S2 are the fittings of the rise (recovery) of the GSB signal. The recovery fitted by a single exponential function is almost the same, with a time constant of 2.1 and 2.7 ps^{-1} for 6 and 12 × 10^{-5} mM, respectively. The Ag^+ concentrations used were very low (10^{-5} to 10^{-4} mM) to avoid any possible deposition of Ag^0 in the reactor. This concentration, while very low, is still 10−20 times higher than the number of surface Ti atoms of the single crystal.

Figure 1 presents the decay of excited electrons with energies between 1.7 and 1.4 eV. The trace is at 840 nm.

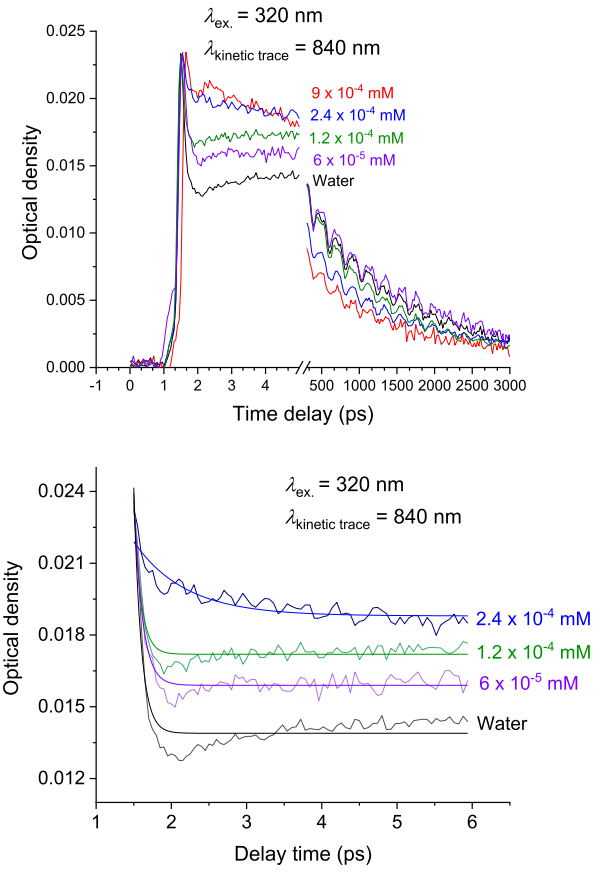

Figure 1. TAS signal from a rutile TiO_2(110) single crystal at 840 nm as a function of time in the presence of Ag^+ at the indicated concentrations. (a) From 0 to 3500 ps and (b) from 0 to 6 ps. Note that the effect of the Ag^+ is inverted at a longer time when compared to the initial short lifetime (<10 ps).

Although small variations do exist from one trace to the next,[17] they are not expected to affect the outcome of the analysis in the present context. At a very short time (<10 ps), the signal decay is slowed down by increasing the concentration of Ag^+, while at a longer time (>300 ps), the situation is reversed. Previously, we modeled the decay of similar single crystals in air[18] and under nitrogen.[19] The signal originates from trapped electrons upon de-excitation from the CB to trap centers. During the measurements, these trapped electrons acquire energy and return to the CB before decaying back to the traps. Self-trapped electrons (polarons) have small energy (typically below 1 eV) and are termed "small polarons"[20,21] in the rutile TiO_2 (as opposed to "large polarons"[22] in the anatase TiO_2).

There are also surface traps that are located on the Ti cations in the terraces and at the step edges, where, in this case, trapped electrons are less mobile. This is in addition to bulk traps, Ti^{x+} cations ($x < 4$).[23] The fact that the presence of Ag^+ affects the first decay may indicate that this latter is largely related to the surface. Part of this signal would be linked to polarons since they are affected by adsorbates [such as CO,[24] water,[25] or carboxylic acids[26] on TiO_2(110)].

Figure 2A shows the computed time constants for both decays with Ag^+ concentrations. The opposite trend is clear. The oscillation of the signal (Figure 1) with time is not noise and has been seen on single crystals[27,28] and well-defined thin films[29] by others. It is related to the excited electrons coupling with lattice vibration in the excited state, and its frequency and amplitude are a function of numerous parameters including the

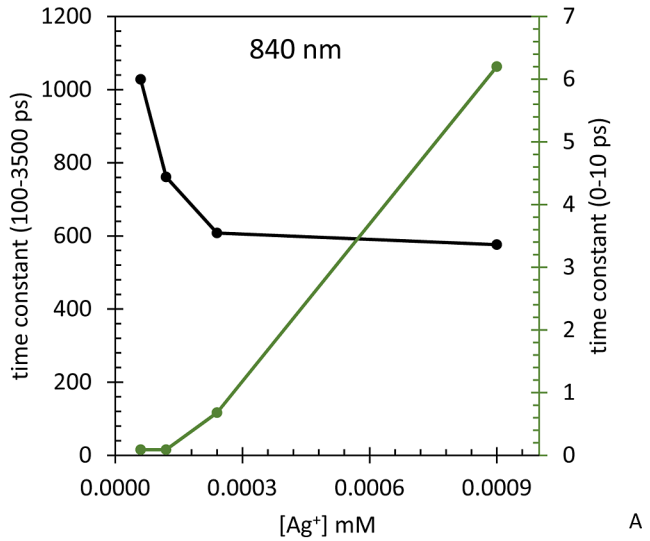

Figure 2. Time constants extracted from the single exponential fitting of the TAS signal at 840 nm at the given Ag^+ concentrations. The time constants for the long-life signal (left *Y*-axis) decrease with increasing Ag^+, while they are reversed for the short-life signal (right *Y*-axis). (B) Change in the time constant with the amplitude of the oscillation wave in the 200−1000 nm region in the presence of four different Ag^+ concentrations. The inset is a sketch of the principle behind the oscillation and a possible explanation for the change in the oscillation wave in the presence of Ag^+. The numbers 1, 2, 3, and 4 are for the Ag^+ concentrations (0.6, 1.2, 2.4, and 9 × 10^{-4} mM, respectively).

probe and pump light frequencies ($\omega = 2nV_sk_{pr}$); n: refractive index, V_s: longitudinal sound velocity, and k_{pr}: wave vector of the probe. While our probe light is too broad to extract quantitative parameters, the periodicity of the oscillation (220 ps) was found to be the same in water and when Ag^+ was present at different concentrations. However, the amplitude of the oscillation decreased with increasing [Ag^+] (Figures S3 and 2b). The relationship between the amplitude and coherent acoustic phonon (CAP) oscillations at a given set of conditions is represented by a damped harmonic oscillator equation.

$$R_{CAP} = A_{Ph}\, e^{-t/\tau} \cos[(\omega + \beta t)t + \varphi]$$

where A_{ph} denotes the amplitude of coherent oscillation, ω is the oscillation frequency of CAPs, α is the chirp coefficient, φ is the initial phase, and τ is approximated by the TAS-obtained time constant. The oscillation is due to the deformation of the crystal during the pump−probe experiment. The deformation potential has been well explained by others.[30,31] In brief, the relative displacement of atoms in the crystal results in strain. This in turn regulates the orbital overlap and therefore induces an electron energy level (δU) shift. When charges propagate in the crystal upon light excitation (excited electrons and holes), their local density at a specific energy level is changed, which leads to changes in the bond energy from which some phonons are generated and others are annihilated. The decrease in the time constant of the long-lived signal is plotted as a function of the amplitude for the four [Ag^+] (Figure 2B). The reciprocal relationship may be explained by the decreasing population of excited electrons in the CB because the higher the [Ag^+], the more electron transfer would occur.

Figure 3 presents the visible light signal attributed to holes, while Table 1 gives the fitted parameters. Although some

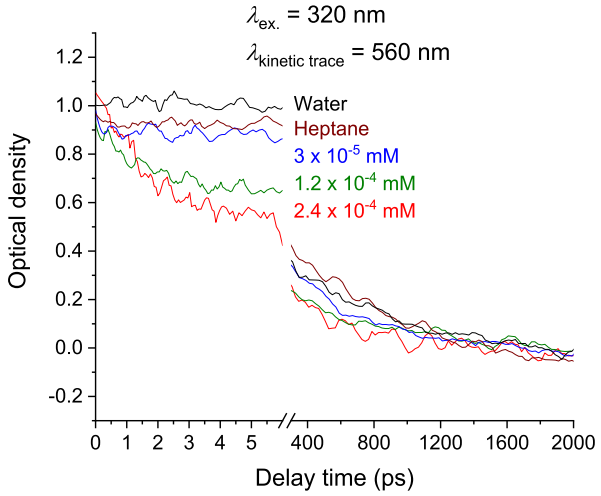

Figure 3. TAS signal from a rutile TiO_2(110) single crystal at 560 nm as a function of time in the presence of Ag^+ at the indicated concentrations. Note that the effect of Ag^+ on the signal is the same at a longer time when compared to the initial short lifetime.

overlap with excited electrons exists,[32] the decay of the signal with increasing wavelengths from 400 to 550 nm may indicate that hole contribution largely decreases with increasing wavelengths. Holes residing on O atoms typically have energy[33] between 2 and 2.5 eV. The signal originates from those trapped holes absorbing visible light energy and is then detrapped, increasing their mobility. This may be viewed as

Table 1. Parameters of the Bi-Exponential Function Used to Fit the Trace Signal at 560 nm of a Rutile TiO_2 (110) Single Crystal in Water and an Aqueous Solution Containing Ag^+ at the Indicated Concentrations

	water	3×10^{-5} mM	6×10^{-5} mM	1.2×10^{-4} mM	2.4×10^{-4} mM
A_1	0.92	0.54	0.58	3.3	3.1
τ_1	118	153	71	1.84	1.9
A_2	0.85	0.48	0.34	0.64	0.5
τ_2	896	841	775	330	382
$<\tau>$	799	724	680	321	371

becoming holes in the VB again, with the extra energy dissipated. In Figure 3, the spectra are smoothed (5 points) because typically the signal in this region is noisier than that in the IR region. As can be seen, the decay time is faster with increasing $[Ag^+]$.

Scheme 1 presents a diagram with an attempt to explain the observations. In the absence of light, Ag^+ interacts with the TiO_2(110) rutile surface. Because both are in an aqueous environment, the surface is fully hydroxylated and Ag^+ is solvated. Upon hydroxylation, surface defects are healed, and the surface is composed exclusively of Ti^{4+} cations, in-plane oxygen atoms, and bridging −OH. The exact coordination of Ag^+ to water molecules is still under study; the most recent work indicates that a Ag^+ is coordinated to two molecules of water in an axial configuration.[34] We will assume that a Ag^+ interacting with the surface has either lost solvation (upon adsorption) or that the presence of water molecules does not affect its mode of interaction (since there is no net charge transfer). Because of the difference in charge, Ag^+ would interact with the surface hydroxyls of TiO_2. We view this as the ground-state configuration (labeled 1 in Scheme 1). Upon light absorption, electrons are transferred to the CB, and holes are formed in the VB. An adsorbed Ag^+ will move from an O atom of surface hydroxyls (hole centers) to Ti^{3+} cations (electron trap). While surface hydroxyls are weak hole traps,[35] they become strong in the presence of water.[36] By doing so, two changes occur in the excited state when Ag^+ is present. First, excited electrons at and near the surface will be attracted to Ag^+ instead of being trapped (either self-trapped or in deep traps). That may explain the increase in the time constant of the TAS IR signal over a short lifetime. Second, holes will be pushed away because of a repulsion with the ions (detrapped), increasing their mobility. This would result in decreasing their population in the trapped centers. Both effects are poised to increase the electron transfer rate. Excited electrons residing longer in the CB then have higher energy than trapped electrons and are more mobile. This favors the electron transfer rate to make Ag^0. Holes returning to the VB create a higher potential energy difference for electrons from water to be transferred (instead of the less energetic, trapped ones) and, as a result, generate O_2.

Scheme 1. Qualitative Schematic Description of the Energy Events for the Photoreduction of Ag^+ to Ag^0 on a TiO_2(110) Rutile Single Crystal[a]

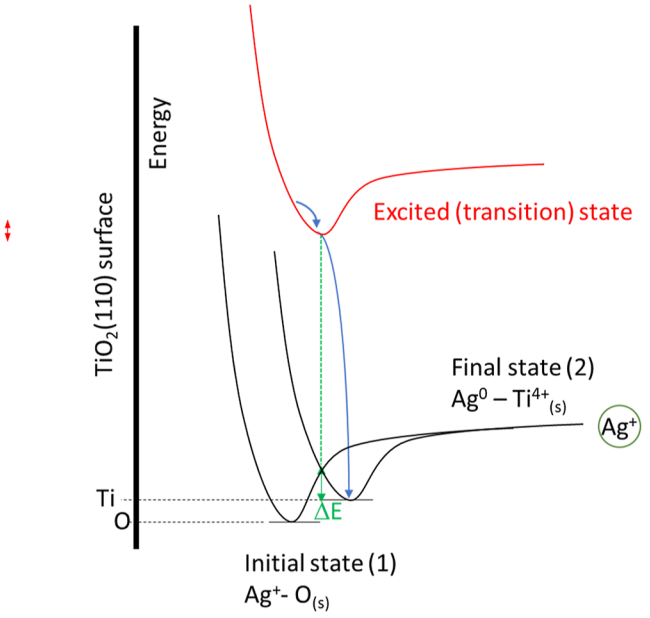

[a] ΔE is the displacement energy of a Ag^+ adsorbed on a surface oxygen (initial state) to Ag^0 on a Ti^{4+} surface (final state) upon acquiring an electron from the CB. In the diagram, the initial state is put at a lower energy because Ag^+−O^{2-} bond energy is stronger than Ag^0−Ti^{4+} bond energy.

Difference from an Organic Adsorbate. Alcohols such as methanol[37] and ethanol[38] or amines such as triethanolamine[39,40] (TEA) are commonly used as hole scavengers in photoreactions for hydrogen production over semiconductor photocatalysts. Their addition results in suppressing the electron−hole recombination rate, allowing for hydrogen ions to be reduced to H_2 by excited electrons transferred to the CB. Work conducted using pump−probe femtosecond spectroscopy has shown, as expected, an increase in the signal attributed to excited electrons when these hole scavenger (electron-donating) molecules are used.[19,41] In the case of alcohols on the TiO_2(110) surface, their dissociative form (alkoxides) has been shown to be more efficient for this electron transfer reaction.[42−44] The alkoxides reside on the Ti^{4+}_{5c} site with a bond made between the O 2p of the alkoxide (alcohol)[45,46] and the empty states of the Ti 3d band. Under photoexcitation, these adsorbates are already in their optimal ground-state position to participate in the electron transfer events (Scheme 2) and therefore do not change sites. This is different from the case of a metal ion (in this case, Ag^+), where it interacts with the surface oxygen anions in the absence of photons. Scheme 2 presents a comparison between both cases: a Ag^+ ion as an electron scavenger and a primary alcohol (ethanol in this case) as a hole scavenger.

The results obtained on Ag^+ cations are similar to those found for Ce^{4+} cations[47] also on the same surface, TiO_2(110) (in this case, Ce^{4+} is ultimately reduced to Ce^{3+}, also as electron scavengers). The analysis in this work as well as for Ce^{4+} interaction with the same surface[47] does not take into consideration the possible role of the counterion (NO_3^-) in the case of Ag^+ and $[(NH_4^+)_2(NO_3^-)_6]^{4-}$ in the case of Ce^{4+}. It appears, based on the results of these two metal cations, that their presence increases the charge accumulation of the excited

Scheme 2. Schematic Representation of the Interaction of Ag^+ (A) and Dissociatively Adsorbed Ethanol (B) with the Surface of TiO_2(110) before and after Photoexcitation[a]

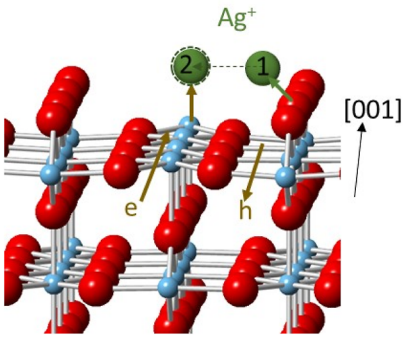

(A)

Initial state: Ag^+ interaction with high electron density sites (O_{3c} or O_{2c} atoms).

- Upon light excitation, *e* are transferred from O2p to Ti3d. In an aqueous environment the surface is hydroxylated (hydroxyls are omitted in the figure).This is viewed as from O2p of the HO_{2c} to the Ti_{5c} resulting in Ti_{5c}^{3+} and an $HO^{\cdot}{}_{2c}$ radical.
- The creation of holes on the $O_{2c,3c}$ sites repels Ag^+ which are then attracted to the Ti_{5c}^{3+} sites.
- As a consequence, *h* become more mobile while *e* are directed toward the Ag^+ instead of being trapped.

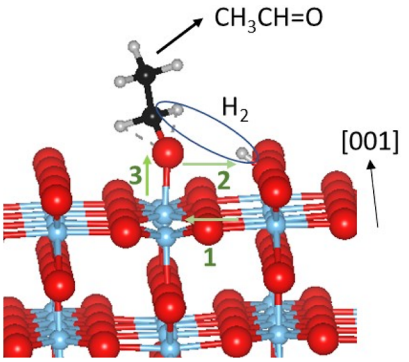

(B)

Initial state: dissociative adsorption (ethoxy) – the bond between the O2p and Ti3d is a dative bond.

- Upon light excitation, *e* are transferred from O2p to Ti3d (1). This is viewed as from O2p of the HO_{2c} to the Ti_{5c} resulting in Ti_{5c}^{3+} and an $HO^{\cdot}{}_{2c}$ radical.
- The alkoxy donates an *e* to the $HO^{\cdot}{}_{2c}$ radical and a second electron to the Ti3d band (current doubling[45]) (2). This results in the breaking of one C-H bond closest to the alkoxy O atom (beta-hydride elimination).
- The O atom of the alkoxy recuperates the two *e* involved, initially in the bonding with Ti, to make the second bond with the C (C=O) and generates the product (acetaldehyde[19]).

The repulsion between the Ti^{3+} and O2p of the alkoxy at the excited state leading to the formation of acetaldehyde can be explained without the need for surface migration from one site to the other.

[a] Ag^+ is an electron trap, while ethanol (like other alcohols) is a hole trap. *h*: hole(s) and *e*: electron(s). (B) is constructed from an energy-minimized structure of a TiO_2(110) slab and ethanol, see ref 46 for more details, while (A) is a schematic representation.

electrons on the surface, increasing (initially) their lifetime instead of being decayed in trap sites.

CONCLUSIONS

In conclusion, the interaction of Ag^+ with the TiO_2(110) surface under UV light excitation resulted in four observations. (1) The appearance of GSB due to the suppression of a large fraction of the de-excitation route (CB electrons → VB) in the presence of Ag^+. (2) A slower decay with time of excited electrons (in the 0 to 10 ps) with increasing [Ag^+]. (3) A decrease in the amplitude of the acoustic oscillation with increasing [Ag^+]. (4) A faster decay with time of the visible light signal, largely attributed to trapped holes, with increasing [Ag^+]. Schematics discussing these events in which Ag^+ moves from one site (a surface O atom) to another (a surface Ti atom) are proposed. These observations related to the interaction of metal cations with an excited oxide semiconductor surface might be more general because a similar behavior is observed for Ce^{4+} cations' interaction with the TiO_2(110) surface.[47]

AUTHOR INFORMATION

Corresponding Author

H. **Idriss** – *Institute of Functional Interfaces (IFG), Karlsruhe Institute of Technology (KIT), 76344 Eggenstein-Leopoldshafen, Germany;* orcid.org/0000-0001-8614-7019; Email: hicham.idriss@kit.edu

Author

K. Katsiev – *Surface Science and Advanced Characterization, SABIC-CRD at KAUST, Thuwal 23955, Saudi Arabia*

Notes

The authors declare no competing financial interest.

ACKNOWLEDGMENTS

H.I. thanks Dr. Christoph Rohmann (NIST, USA) for conducting the DFT + U study of ethanol on the TiO_2(110) surface, previously published.[46]

REFERENCES

(1) Marcus, R. A. Electron transfer react in chemistry. Theory and experiment. *Pure Appl. Chem.* **1997**, *69*, 13–29.

(2) Kolasinski, K. W.; Gogola, J. W.; Barclay, W. B. Test of Marcus Theory Predictions for Electroless Etching of Silicon. *J. Phys. Chem. C* **2012**, *116*, 21472−21481.
(3) Das, A.; Kamatham, N.; Mohan Raj, A.; Sen, P.; Ramamurthy, V. Marcus Relationship Maintained During Ultrafast Electron Transfer Across a Supramolecular Capsular Wall. *J. Phys. Chem. A* **2020**, *124*, 5297−5305.
(4) Muir, J. M. R.; Idriss, H. Computational study of cysteine interaction with the rutile TiO_2(110) surface. *Surf. Sci.* **2013**, *617*, 60−67.
(5) Ren, X.; Wang, C.-C.; Li, Y.; Wang, C.-Y.; Wang, P.; Gao, S. Ag(I) removal and recovery from wastewater adopting NH_2-MIL-125 as efficient adsorbent: A 3Rs (reduce, recycle and reuse) approach and practice. *Chem. Eng. J.* **2022**, *442*, 136306.
(6) Fujishima, A.; Rao, T. N.; Tryk, D. A. Titanium dioxide photocatalysis. *J. Photochem. Photobiol., C* **2000**, *1*, 1−21.
(7) Onda, K.; Li, B.; Zhao, J.; Jordan, K. D.; Yang, J.; Petek, H. Wet Electrons at the H $_2$ O/TiO $_2$ (110) Surface. *Science* **2005**, *308*, 1154−1158.
(8) Triggiani, L.; Brunetti, A.; Aloi, A.; Comparelli, R.; Curri, M. L.; Agostiano, A.; Striccoli, M.; Tommasi, R. Excitation-Dependent Ultrafast Carrier Dynamics of Colloidal TiO_2 Nanorods in Organic Solvent. *J. Phys. Chem. C* **2014**, *118*, 25215−25222.
(9) Fu, Z.; Onishi, H. Infrared and Near-Infrared Spectrometry of Anatase and Rutile Particles Bandgap Excited in Liquid. *J. Phys. Chem. B* **2023**, *127*, 321−327.
(10) Lun Pang, C.; Lindsay, R.; Thornton, G. Chemical reactions on rutile TiO_2(110). *Chem. Soc. Rev.* **2008**, *37*, 2328−2353.
(11) Berger, O. Understanding the fundamentals of TiO_2 surfaces Part II. Reactivity and surface chemistry of TiO_2 single crystals. *Surf. Eng.* **2022**, *38*, 846−906.
(12) Williams, O. B. J.; Katsiev, K.; Baek, B.; Harrison, G.; Thornton, G.; Idriss, H. Direct Visualization of a Gold Nanoparticle Electron Trapping Effect. *J. Am. Chem. Soc.* **2022**, *144* (2), 1034−1044.
(13) Gao, Z.; Leng, C.; Zhao, H.; Wei, X.; Shi, H. Z.; Xiao, Z. The Electrical Behaviors of Grain Boundaries in Polycrystalline Optoelectronic Materials. *Adv. Mater.* **2024**, *36*, 2304855.
(14) Wahab, A. K.; Ould-Chikh, S.; Meyer, K.; Idriss, H. On the "possible" synergism of the different phases of TiO2 in photo-catalysis for hydrogen production. *J. Catal.* **2017**, *352*, 657−671.
(15) Wilson, J. N.; Idriss, H. Structure-Sensitivity and Photocatalytic Reactions of Semiconductors. Effect of the Last Layer Atomic Arrangement. *J. Am. Chem. Soc.* **2002**, *124*, 11284−11285.
(16) Kudo, A.; Miseki, Y. Heterogeneous photocatalyst materials for water splitting. *Chem. Soc. Rev.* **2009**, *38*, 253−278.
(17) Al-Amoudi, M.; Katsiev, K.; Idriss, H. Monitoring the lifetime of photoexcited electrons in a fresh and bulk reduced rutile TiO_2 single crystal. Possible Anisotropic Propagation. *J. Phys. Chem. Lett.* **2023**, *14*, 9238−9244.
(18) Maity, P.; Mohammed, O. F.; Katsiev, K.; Idriss, H. Study of the Bulk Defect Mediated Photoexcited Charge Recombination in Anatase and Rutile TiO_2 Single Crystals by Femtosecond Time-Resolved Spectroscopy. *J. Phys. Chem. C* **2018**, *122*, 8925−8932.
(19) Katsiev, K.; Harrison, G. T.; Al-Salik, Y.; Thornton, G.; Idriss, H. Gold Cluster Coverage Effect on H2 Production over Rutile TiO_2(110). *ACS Catal.* **2019**, *9*, 8294−8305.
(20) Reticcioli, M.; Setvin, M.; Schmid, M.; Diebold, U.; Franchini, C. Formation and dynamics of small polarons on the rutile TiO_2(110) surface. *Phys. Rev. B* **2018**, *98*, 045306.
(21) Yang, S.; Brant, A. T.; Giles, N. C.; Halliburton, L. E. Intrinsic small polarons in rutile TiO_2. *Phys. Rev. B* **2013**, *87*, 125201.
(22) Elmaslmane, A. R.; Watkins, M. B.; McKenna, K. P. First-Principles Modeling of Polaron Formation in TiO_2 Polymorphs. *J. Chem. Theory Comput.* **2018**, *14*, 3740−3751.
(23) Finazzi, E.; Di Valentin, C.; Pacchioni, G. Nature of Ti Interstitials in Reduced Bulk Anatase and Rutile TiO_2. *J. Phys. Chem. C* **2009**, *113*, 3382−3385.
(24) Cheng, C.; Zhu, Y.; Fang, W.-H.; Long, R.; Prezhdo, O. V. CO Adsorbate Promotes Polaron Photoactivity on the Reduced Rutile TiO_2(110) Surface. *JACS Au* **2022**, *2*, 234−245.
(25) Gao, C.; Zhang, L.; Zheng, Q.; Zhao, J. Tuning the Lifetime of Photoexcited Small Polarons on Rutile TiO_2 Surface via Molecular Adsorption. *J. Phys. Chem. C* **2021**, *125* (49), 27275−27282.
(26) Tanner, A. J.; Wen, B.; Ontaneda, J.; Zhang, Y.; Grau-Crespo, R.; Fielding, H. H.; Selloni, A.; Thornton, G. Polaron-Adsorbate Coupling at the TiO_2(110)-Carboxylate Interface. *J. Phys. Chem. Lett.* **2021**, *12* (14), 3571−3576.
(27) Shih, H. C.; Chen, L. Y.; Luo, C. W.; Wu, K. H.; Lin, J.-Y.; Juang, J. Y.; Uen, T. M.; Lee, J. M.; Chen, J. M.; Kobayashi, T. Ultrafast thermoelastic dynamics of $HoMnO_3$ single crystals derived from femtosecond optical pump−probe spectroscopy. *New J. Phys.* **2011**, *13*, 053003.
(28) Wu, S.; Geiser, P.; Jun, J.; Karpinski, J.; Sobolewski, R. Femtosecond optical generation and detection of coherent acoustic phonons in GaN single crystals. *Phys. Rev. B* **2007**, *76* (8), 085210.
(29) Ren, Y. H.; Trigo, M.; Merlin, R.; Adyam, V.; Li, Q. Generation and detection of coherent longitudinal acoustic phonons in the La0.67Sr0.33MnO3 thin films by femtosecond light pulses. *Appl. Phys. Lett.* **2007**, *90*, 251918.
(30) Ma, X.-R.; Li, Y.-C.; Ge, C.; Wang, P.; Song, H.-Y.; Liu, S.-B. Ultrafast generation and detection of coherent acoustic phonons in SnS0.91Se0.09. *Results Phys.* **2023**, *45*, 106241.
(31) Ruello, P.; Gusev, V. E. Physical mechanisms of coherent acoustic phonons generation by ultrafast laser action. *Ultrasonics* **2015**, *56*, 21−35.
(32) Yoshihara, T.; Katoh, R.; Furube, A.; Tamaki, Y.; Murai, M.; Hara, K.; Murata, S.; Arakawa, H.; Tachiya, M. Identification of Reactive Species in Photoexcited Nanocrystalline TiO_2 Films by Wide-Wavelength-Range (400−2500 nm) Transient Absorption Spectroscopy. *J. Phys. Chem. B* **2004**, *108*, 3817−3823.
(33) Ji, Y.; Wang, B.; Luo, Y. Location of Trapped Hole on Rutile-TiO_2(110) Surface and Its Role in Water Oxidation. *J. Phys. Chem. C* **2012**, *116*, 7863−7866.
(34) Busato, M.; Melchior, A.; Migliorati, V.; Colella, A.; Persson, I.; Mancini, G.; Veclani, D.; D'Angelo, P. Elusive Coordination of the Ag^+ Ion in Aqueous Solution: Evidence for a Linear Structure. *Inorg. Chem.* **2020**, *59*, 17291−17302.
(35) Fazio, G.; Ferrighi, L.; Di Valentin, C. Photoexcited carriers recombination and trapping in spherical vs faceted TiO2 nanoparticles. *Nano Energy* **2016**, *27*, 673−689.
(36) Shirai, K.; Fazio, G.; Sugimoto, T.; Selli, D.; Ferraro, L.; Watanabe, K.; Haruta, M.; Ohtani, B.; Kurata, H.; Di Valentin, C.; Matsumoto, Y. Water-Assisted Hole Trapping at the Highly Curved Surface of Nano-TiO_2 Photocatalyst. *J. Am. Chem. Soc.* **2018**, *140*, 1415−1422.
(37) Mills, A.; Bingham, M.; O'Rourke, C.; Bowker, M. Modelled kinetics of the rate of hydrogen evolution as a function of metal catalyst loading in the photocatalysed reforming of methanol by Pt (or Pd)/TiO_2. *J. Photochem. Photobiol., A* **2019**, *373*, 122−130.
(38) Murdoch, M.; Waterhouse, G. I. N.; Nadeem, M. A.; Metson, J. B.; Keane, M. A.; Howe, R. F.; Llorca, J.; Idriss, H. Effect of gold loading and particle size on photo-catalytic hydrogen production from ethanol over Au/TiO_2 anatase and rutile nanoparticles. *Nat. Chem.* **2011**, *3*, 489−492.
(39) Schneider, J.; Matsuoka, M.; Takeuchi, M.; Zhang, J.; Horiuchi, Y.; Anpo, M.; Bahnemann, D. W. Understanding TiO_2 Photocatalysis: Mechanisms and Materials. *Chem. Rev.* **2014**, *114* (19), 9919−9986.
(40) Khan, M. A.; Maity, P.; Al-Oufi, M.; AlHowaish, I. K.; Idriss, H. Electron Transfer of the Metal/Semiconductor System in Photocatalysis. *J. Phys. Chem. C* **2018**, *122*, 16779−16787.
(41) Yamakata, A.; Vequizo, J. J. M.; Matsunaga, H. Distinctive Behavior of Photogenerated Electrons and Holes in Anatase and Rutile TiO_2 Powders. *J. Phys. Chem. C* **2015**, *119*, 24538−24545.
(42) Muir, J. N.; Choi, Y. M.; Idriss, H. Computational study of ethanol adsorption and reaction over rutile TiO_2(110) surfaces. *Phys. Chem. Chem. Phys.* **2012**, *14*, 11910−11919.

(43) Di Valentin, C.; Fittipaldi, D. Hole Scavenging by Organic Adsorbates on the TiO_2 Surface: A DFT Model Study. *J. Phys. Chem. Lett.* **2013**, *4*, 1901−1906.
(44) Chu, W.; Tan, S.; Zheng, Q.; Fang, W.; Feng, Y.; Prezhdo, O. V.; Wang, B.; Li, X.-Z.; Zhao, J. Ultrafast charge transfer coupled to quantum proton motion at molecule/metal oxide interface. *Sci. Adv.* **2022**, *8*, No. eabo2675.
(45) Huo, P.; Hansen, J. Ø.; Martinez, U.; Lira, E.; Streber, R.; Wei, Y.; Lægsgaard, E.; Hammer, B.; Wendt, S.; Besenbacher, F. Ethanol Diffusion on Rutile TiO_2(110) Mediated by H Adatoms. *J. Phys. Chem. Lett.* **2012**, *3* (3), 283−288.
(46) Rohmann, C.; Idriss, H. A computational study of the interaction of oxygenates with the surface of rutile TiO_2(110). Structural and electronic trends. *J. Phys.: Condens.Matter* **2022**, *34*, 154002.
(47) Katsiev, K.; Idriss, H. Study of rutile TiO_2(110) single crystal by transient absorption spectroscopy in the presence of Ce^{4+} cations in aqueous environment. Implication on water splitting. *J. Phys.: Condens.Matter* **2024**, *36*, 325002.